Search for an invisible muon philic scalar X_0 or vector X_1 via $J/\psi \to \mu^+\mu^- +$ invisible decay at BESIII

M. Ablikim[1], M. N. Achasov[4,b], P. Adlarson[75], O. Afedulidis[3], X. C. Ai[80], R. Aliberti[35], A. Amoroso[74A,74C], M. R. An[39], Q. An[71,58], Y. Bai[57], O. Bakina[36], I. Balossino[29A], Y. Ban[46,g], H.-R. Bao[63], V. Batozskaya[1,44], K. Begzsuren[32], N. Berger[35], M. Berlowski[44], M. Bertani[28A], D. Bettoni[29A], F. Bianchi[74A,74C], E. Bianco[74A,74C], A. Bortone[74A,74C], I. Boyko[36], R. A. Briere[5], A. Brueggemann[68], H. Cai[76], X. Cai[1,58], A. Calcaterra[28A], G. F. Cao[1,63], N. Cao[1,63], S. A. Cetin[62A], J. F. Chang[1,58], W. L. Chang[1,63], G. R. Che[43], G. Chelkov[36,a], C. Chen[43], Chao Chen[55], G. Chen[1], H. S. Chen[1,63], M. L. Chen[1,58,63], S. J. Chen[42], S. L. Chen[45], S. M. Chen[61], T. Chen[1,63], X. R. Chen[31,63], X. T. Chen[1,63], Y. B. Chen[1,58], Y. Q. Chen[34], Z. J. Chen[25,h], S. K. Choi[10A], X. Chu[43], G. Cibinetto[29A], S. C. Coen[3], F. Cossio[74C], J. J. Cui[50], H. L. Dai[1,58], J. P. Dai[78], A. Dbeyssi[18], R. E. de Boer[3], D. Dedovich[36], Z. Y. Deng[1], A. Denig[35], I. Denysenko[36], M. Destefanis[74A,74C], F. De Mori[74A,74C], B. Ding[66,1], X. X. Ding[46,g], Y. Ding[34], Y. Ding[40], J. Dong[1,58], L. Y. Dong[1,63], M. Y. Dong[1,58,63], X. Dong[76], M. C. Du[1], S. X. Du[80], Z. H. Duan[42], P. Egorov[36,a], Y. H. Fan[45], J. Fang[1,58], S. S. Fang[1,63], W. X. Fang[1], Y. Fang[1], Y. Q. Fang[1,58], R. Farinelli[29A], L. Fava[74B,74C], F. Feldbauer[3], G. Felici[28A], C. Q. Feng[71,58], J. H. Feng[59], Y. T. Feng[71,58], K Fischer[69], M. Fritsch[3], C. D. Fu[1], J. L. Fu[63], Y. W. Fu[1], H. Gao[63], Y. N. Gao[46,g], Yang Gao[71,58], S. Garbolino[74C], I. Garzia[29A,29B], P. T. Ge[76], Z. W. Ge[42], C. Geng[59], E. M. Gersabeck[67], A Gilman[69], K. Goetzen[13], L. Gong[40], W. X. Gong[1,58], W. Gradl[35], S. Gramigna[29A,29B], M. Greco[74A,74C], M. H. Gu[1,58], Y. T. Gu[15], C. Y Guan[1,63], Z. L. Guan[22], A. Q. Guo[31,63], L. B. Guo[41], M. J. Guo[50], R. P. Guo[49], Y. P. Guo[12,f], A. Guskov[36,a], J. Gutierrez[27], K. L. Han[63], T. T. Han[1], W. Y. Han[39], X. Q. Hao[19], F. A. Harris[65], K. K. He[55], K. L. He[1,63], F. H. Heinsius[3], C. H. Heinz[35], Y. K. Heng[1,58,63], C. Herold[60], T. Holtmann[3], P. C. Hong[12,f], G. Y. Hou[1,63], X. T. Hou[1,63], Y. R. Hou[63], Z. L. Hou[1], B. Y. Hu[59], H. M. Hu[1,63], J. F. Hu[56,i], T. Hu[1,58,63], Y. Hu[1], G. S. Huang[71,58], K. X. Huang[59], L. Q. Huang[31,63], X. T. Huang[50], Y. P. Huang[1], T. Hussain[73], F. Hölzken[3], N Hüsken[27,35], N. in der Wiesche[68], M. Irshad[71,58], J. Jackson[27], S. Jaeger[3], S. Janchiv[32], J. H. Jeong[10A], Q. Ji[1], Q. P. Ji[19], X. B. Ji[1,63], X. L. Ji[1,58], Y. Y. Ji[50], X. Q. Jia[50], Z. K. Jia[71,58], H. B. Jiang[76], P. C. Jiang[46,g], S. S. Jiang[39], T. J. Jiang[16], X. S. Jiang[1,58,63], Y. Jiang[63], J. B. Jiao[50], Z. Jiao[23], S. Jin[42], Y. Jin[66], M. Q. Jing[1,63], X. M. Jing[63], T. Johansson[75], X. K.[1], S. Kabana[33], N. Kalantar-Nayestanaki[64], X. L. Kang[9], X. S. Kang[40], M. Kavatsyuk[64], B. C. Ke[80], V. Khachatryan[27], A. Khoukaz[68], R. Kiuchi[1], O. B. Kolcu[62A], B. Kopf[3], M. Kuessner[3], A. Kupsc[44,75], W. Kühn[37], J. J. Lane[67], P. Larin[18], L. Lavezzi[74A,74C], T. T. Lei[71,58], Z. H. Lei[71,58], H. Leithoff[35], M. Lellmann[35], T. Lenz[35], C. Li[43], C. Li[47], C. H. Li[39], Cheng Li[71,58], D. M. Li[80], F. Li[1,58], G. Li[1], H. Li[71,58], H. B. Li[1,63], H. J. Li[19], H. N. Li[56,i], Hui Li[43], J. R. Li[61], J. S. Li[59], Ke Li[1], L. J Li[1,63], L. K. Li[1], Lei Li[48], M. H. Li[43], P. R. Li[38,k], Q. X. Li[50], S. X. Li[12], T. Li[50], W. D. Li[1,63], W. G. Li[1], X. H. Li[71,58], X. L. Li[50], Xiaoyu Li[1,63], Y. G. Li[46,g], Z. J. Li[59], Z. X. Li[15], C. Liang[42], H. Liang[1,63], H. Liang[71,58], Y. F. Liang[54], Y. T. Liang[31,63], G. R. Liao[14], L. Z. Liao[50], Y. P. Liao[1,63], J. Libby[26], A. Limphirat[60], D. X. Lin[31,63], T. Lin[1], B. J. Liu[1], B. X. Liu[76], C. Liu[34], C. X. Liu[1], F. H. Liu[53], Fang Liu[1], Feng Liu[6], G. M. Liu[56,i], H. Liu[38,j,k], H. B. Liu[15], H. M. Liu[1,63], Huanhuan Liu[1], Huihui Liu[21], J. B. Liu[71,58], J. Y. Liu[1,63], K. Liu[38,j,k], K. Y. Liu[40], Ke Liu[22], L. Liu[71,58], L. C. Liu[43], Lu Liu[43], M. H. Liu[12,f], P. L. Liu[1], Q. Liu[63], S. B. Liu[71,58], T. Liu[12,f], W. K. Liu[43], W. M. Liu[71,58], X. Liu[38,j,k], Y. Liu[80], Y. Liu[38,j,k], Y. B. Liu[43], Z. A. Liu[1,58,63], Z. Q. Liu[50], X. C. Lou[1,58,63], F. X. Lu[59], H. J. Lu[23], J. G. Lu[1,58], X. L. Lu[1], Y. Lu[7], Y. P. Lu[1,58], Z. H. Lu[1,63], C. L. Luo[41], M. X. Luo[79], T. Luo[12,f], X. L. Luo[1,58], X. R. Lyu[63], Y. F. Lyu[43], F. C. Ma[40], H. Ma[78], H. L. Ma[1], J. L. Ma[1,63], L. L. Ma[50], M. M. Ma[1,63], Q. M. Ma[1], R. Q. Ma[1,63], X. Y. Ma[1,58], Y. Ma[46,g], Y. M. Ma[31], F. E. Maas[18], M. Maggiora[74A,74C], S. Malde[69], A. Mangoni[28B], Y. J. Mao[46,g], Z. P. Mao[1], S. Marcello[74A,74C], Z. X. Meng[66], J. G. Messchendorp[13,64], G. Mezzadri[29A], H. Miao[1,63], T. J. Min[42], R. E. Mitchell[27], X. H. Mo[1,58,63], B. Moses[27], N. Yu. Muchnoi[4,b], J. Muskalla[35], Y. Nefedov[36], F. Nerling[18,d], I. B. Nikolaev[4,b], Z. Ning[1,58], S. Nisar[11,l], Q. L. Niu[38,j,k], W. D. Niu[55], Y. Niu [50], S. L. Olsen[63], Q. Ouyang[1,58,63], S. Pacetti[28B,28C], X. Pan[55], Y. Pan[57], A. Pathak[34], P. Patteri[28A], Y. P. Pei[71,58], M. Pelizaeus[3], H. P. Peng[71,58], Y. Y. Peng[38,j,k], K. Peters[13,d], J. L. Ping[41], R. G. Ping[1,63], S. Plura[35], V. Prasad[33], F. Z. Qi[1], H. Qi[71,58], H. R. Qi[61], M. Qi[42], T. Y. Qi[12,f], S. Qian[1,58], W. B. Qian[63], C. F. Qiao[63], J. J. Qin[72], L. Q. Qin[14], X. S. Qin[50], Z. H. Qin[1,58], J. F. Qiu[1], S. Q. Qu[61], C. F. Redmer[35], K. J. Ren[39], A. Rivetti[74C], M. Rolo[74C], G. Rong[1,63], Ch. Rosner[18], S. N. Ruan[43], N. Salone[44], A. Sarantsev[36,c], Y. Schelhaas[35], K. Schoenning[75], M. Scodeggio[29A], K. Y. Shan[12,f], W. Shan[24], X. Y. Shan[71,58], J. F. Shangguan[55], L. G. Shao[1,63], M. Shao[71,58], C. P. Shen[12,f], H. F. Shen[1,63], W. H. Shen[63], X. Y. Shen[1,63], B. A. Shi[63], H. C. Shi[71,58], J. L. Shi[12], J. Y. Shi[1], Q. Q. Shi[55], R. S. Shi[1,63], X. Shi[1,58], J. J. Song[19], T. Z. Song[59], W. M. Song[34,1], Y. J. Song[12], S. Sosio[74A,74C], S. Spataro[74A,74C], F. Stieler[35], Y. J. Su[63], G. B. Sun[76],

G. X. Sun[1], H. Sun[63], H. K. Sun[1], J. F. Sun[19], K. Sun[61], L. Sun[76], S. S. Sun[1,63], T. Sun[51,e], W. Y. Sun[34], Y. Sun[9], Y. J. Sun[71,58], Y. Z. Sun[1], Z. T. Sun[50], Y. X. Tan[71,58], C. J. Tang[54], G. Y. Tang[1], J. Tang[59], Y. A. Tang[76], L. Y Tao[72], Q. T. Tao[25,h], M. Tat[69], J. X. Teng[71,58], V. Thoren[75], W. H. Tian[52], W. H. Tian[59], Y. Tian[31,63], Z. F. Tian[76], I. Uman[62B], Y. Wan[55], S. J. Wang [50], B. Wang[1], B. L. Wang[63], Bo Wang[71,58], C. W. Wang[42], D. Y. Wang[46,g], F. Wang[72], H. J. Wang[38,j,k], J. P. Wang [50], K. Wang[1,58], L. L. Wang[1], M. Wang[50], Meng Wang[1,63], N. Y. Wang[63], S. Wang[12,f], S. Wang[38,j,k], T. Wang[12,f], T. J. Wang[43], W. Wang[59], W. Wang[72], W. P. Wang[71,58], X. Wang[46,g], X. F. Wang[38,j,k], X. J. Wang[39], X. L. Wang[12,f], Y. Wang[61], Y. D. Wang[45], Y. F. Wang[1,58,63], Y. L. Wang[19], Y. N. Wang[45], Y. Q. Wang[1], Yaqian Wang[17], Yi Wang[61], Z. Wang[1,58], Z. L. Wang[72], Z. Y. Wang[1,63], Ziyi Wang[63], D. Wei[70], D. H. Wei[14], F. Weidner[68], S. P. Wen[1], C. Wenzel[3], U. Wiedner[3], G. Wilkinson[69], M. Wolke[75], L. Wollenberg[3], C. Wu[39], J. F. Wu[1,8], L. H. Wu[1], L. J. Wu[1,63], X. Wu[12,f], X. H. Wu[34], Y. Wu[71], Y. H. Wu[55], Y. J. Wu[31], Z. Wu[1,58], L. Xia[71,58], X. M. Xian[39], T. Xiang[46,g], D. Xiao[38,j,k], G. Y. Xiao[42], S. Y. Xiao[1], Y. L. Xiao[12,f], Z. J. Xiao[41], C. Xie[42], X. H. Xie[46,g], Y. Xie[50], Y. G. Xie[1,58], Y. H. Xie[6], Z. P. Xie[71,58], T. Y. Xing[1,63], C. F. Xu[1,63], C. J. Xu[59], G. F. Xu[1], H. Y. Xu[66], Q. J. Xu[16], Q. N. Xu[30], W. Xu[1], W. L. Xu[66], X. P. Xu[55], Y. C. Xu[77], Z. P. Xu[42], Z. S. Xu[63], F. Yan[12,f], L. Yan[12,f], W. B. Yan[71,58], W. C. Yan[80], X. Q. Yan[1], H. J. Yang[51,e], H. L. Yang[34], H. X. Yang[1], Tao Yang[1], Y. Yang[12,f], Y. F. Yang[43], Y. X. Yang[1,63], Yifan Yang[1,63], Z. W. Yang[38,j,k], Z. P. Yao[50], M. Ye[1,58], M. H. Ye[8], J. H. Yin[1], Z. Y. You[59], B. X. Yu[1,58,63], C. X. Yu[43], G. Yu[1,63], J. S. Yu[25,h], T. Yu[72], X. D. Yu[46,g], C. Z. Yuan[1,63], L. Yuan[2], S. C. Yuan[1], Y. Yuan[1,63], Z. Y. Yuan[59], C. X. Yue[39], A. A. Zafar[73], F. R. Zeng[50], S. H. Zeng[72], X. Zeng[12,f], Y. Zeng[25,h], Y. J. Zeng[1,63], X. Y. Zhai[34], Y. C. Zhai[50], Y. H. Zhan[59], A. Q. Zhang[1,63], B. L. Zhang[1,63], B. X. Zhang[1], D. H. Zhang[43], G. Y. Zhang[19], H. Zhang[71], H. C. Zhang[1,58,63], H. H. Zhang[59], H. H. Zhang[34], H. Q. Zhang[1,58,63], H. Y. Zhang[1,58], J. Zhang[59], J. Zhang[80], J. J. Zhang[52], J. L. Zhang[20], J. Q. Zhang[41], J. W. Zhang[1,58,63], J. X. Zhang[38,j,k], J. Y. Zhang[1], J. Z. Zhang[1,63], Jianyu Zhang[63], L. M. Zhang[61], L. Q. Zhang[59], Lei Zhang[42], P. Zhang[1,63], Q. Y. Zhang[39,80], Shuihan Zhang[1,63], Shulei Zhang[25,h], X. D. Zhang[45], X. M. Zhang[1], X. Y. Zhang[50], Y. Zhang[72], Y. Zhang[69], Y. T. Zhang[80], Y. H. Zhang[1,58], Yan Zhang[71,58], Yao Zhang[1], Z. D. Zhang[1], Z. H. Zhang[1], Z. L. Zhang[34], Z. Y. Zhang[76], Z. Y. Zhang[43], G. Zhao[1], J. Y. Zhao[1,63], J. Z. Zhao[1,58], Lei Zhao[71,58], Ling Zhao[1], M. G. Zhao[43], R. P. Zhao[63], S. J. Zhao[80], Y. B. Zhao[1,58], Y. X. Zhao[31,63], Z. G. Zhao[71,58], A. Zhemchugov[36,a], B. Zheng[72], J. P. Zheng[1,58], W. J. Zheng[1,63], Y. H. Zheng[63], B. Zhong[41], X. Zhong[59], H. Zhou[50], L. P. Zhou[1,63], X. Zhou[76], X. K. Zhou[6], X. R. Zhou[71,58], X. Y. Zhou[39], Y. Z. Zhou[12,f], J. Zhu[43], K. Zhu[1], K. J. Zhu[1,58,63], L. Zhu[34], L. X. Zhu[63], S. H. Zhu[70], S. Q. Zhu[42], T. J. Zhu[12,f], W. J. Zhu[12,f], Y. C. Zhu[71,58], Z. A. Zhu[1,63], J. H. Zou[1], J. Zu[71,58]

(BESIII Collaboration)

[1] Institute of High Energy Physics, Beijing 100049, People's Republic of China
[2] Beihang University, Beijing 100191, People's Republic of China
[3] Bochum Ruhr-University, D-44780 Bochum, Germany
[4] Budker Institute of Nuclear Physics SB RAS (BINP), Novosibirsk 630090, Russia
[5] Carnegie Mellon University, Pittsburgh, Pennsylvania 15213, USA
[6] Central China Normal University, Wuhan 430079, People's Republic of China
[7] Central South University, Changsha 410083, People's Republic of China
[8] China Center of Advanced Science and Technology, Beijing 100190, People's Republic of China
[9] China University of Geosciences, Wuhan 430074, People's Republic of China
[10] Chung-Ang University, Seoul, 06974, Republic of Korea
[11] COMSATS University Islamabad, Lahore Campus, Defence Road, Off Raiwind Road, 54000 Lahore, Pakistan
[12] Fudan University, Shanghai 200433, People's Republic of China
[13] GSI Helmholtzcentre for Heavy Ion Research GmbH, D-64291 Darmstadt, Germany
[14] Guangxi Normal University, Guilin 541004, People's Republic of China
[15] Guangxi University, Nanning 530004, People's Republic of China
[16] Hangzhou Normal University, Hangzhou 310036, People's Republic of China
[17] Hebei University, Baoding 071002, People's Republic of China
[18] Helmholtz Institute Mainz, Staudinger Weg 18, D-55099 Mainz, Germany
[19] Henan Normal University, Xinxiang 453007, People's Republic of China
[20] Henan University, Kaifeng 475004, People's Republic of China
[21] Henan University of Science and Technology, Luoyang 471003, People's Republic of China
[22] Henan University of Technology, Zhengzhou 450001, People's Republic of China
[23] Huangshan College, Huangshan 245000, People's Republic of China

[24] Hunan Normal University, Changsha 410081, People's Republic of China
[25] Hunan University, Changsha 410082, People's Republic of China
[26] Indian Institute of Technology Madras, Chennai 600036, India
[27] Indiana University, Bloomington, Indiana 47405, USA
[28] INFN Laboratori Nazionali di Frascati , (A)INFN Laboratori Nazionali di Frascati, I-00044, Frascati, Italy; (B)INFN Sezione di Perugia, I-06100, Perugia, Italy; (C)University of Perugia, I-06100, Perugia, Italy
[29] INFN Sezione di Ferrara, (A)INFN Sezione di Ferrara, I-44122, Ferrara, Italy; (B)University of Ferrara, I-44122, Ferrara, Italy
[30] Inner Mongolia University, Hohhot 010021, People's Republic of China
[31] Institute of Modern Physics, Lanzhou 730000, People's Republic of China
[32] Institute of Physics and Technology, Peace Avenue 54B, Ulaanbaatar 13330, Mongolia
[33] Instituto de Alta Investigación, Universidad de Tarapacá, Casilla 7D, Arica 1000000, Chile
[34] Jilin University, Changchun 130012, People's Republic of China
[35] Johannes Gutenberg University of Mainz, Johann-Joachim-Becher-Weg 45, D-55099 Mainz, Germany
[36] Joint Institute for Nuclear Research, 141980 Dubna, Moscow region, Russia
[37] Justus-Liebig-Universitaet Giessen, II. Physikalisches Institut, Heinrich-Buff-Ring 16, D-35392 Giessen, Germany
[38] Lanzhou University, Lanzhou 730000, People's Republic of China
[39] Liaoning Normal University, Dalian 116029, People's Republic of China
[40] Liaoning University, Shenyang 110036, People's Republic of China
[41] Nanjing Normal University, Nanjing 210023, People's Republic of China
[42] Nanjing University, Nanjing 210093, People's Republic of China
[43] Nankai University, Tianjin 300071, People's Republic of China
[44] National Centre for Nuclear Research, Warsaw 02-093, Poland
[45] North China Electric Power University, Beijing 102206, People's Republic of China
[46] Peking University, Beijing 100871, People's Republic of China
[47] Qufu Normal University, Qufu 273165, People's Republic of China
[48] Renmin University of China, Beijing 100872, People's Republic of China
[49] Shandong Normal University, Jinan 250014, People's Republic of China
[50] Shandong University, Jinan 250100, People's Republic of China
[51] Shanghai Jiao Tong University, Shanghai 200240, People's Republic of China
[52] Shanxi Normal University, Linfen 041004, People's Republic of China
[53] Shanxi University, Taiyuan 030006, People's Republic of China
[54] Sichuan University, Chengdu 610064, People's Republic of China
[55] Soochow University, Suzhou 215006, People's Republic of China
[56] South China Normal University, Guangzhou 510006, People's Republic of China
[57] Southeast University, Nanjing 211100, People's Republic of China
[58] State Key Laboratory of Particle Detection and Electronics, Beijing 100049, Hefei 230026, People's Republic of China
[59] Sun Yat-Sen University, Guangzhou 510275, People's Republic of China
[60] Suranaree University of Technology, University Avenue 111, Nakhon Ratchasima 30000, Thailand
[61] Tsinghua University, Beijing 100084, People's Republic of China
[62] Turkish Accelerator Center Particle Factory Group, (A)Istinye University, 34010, Istanbul, Turkey; (B)Near East University, Nicosia, North Cyprus, 99138, Mersin 10, Turkey
[63] University of Chinese Academy of Sciences, Beijing 100049, People's Republic of China
[64] University of Groningen, NL-9747 AA Groningen, The Netherlands
[65] University of Hawaii, Honolulu, Hawaii 96822, USA
[66] University of Jinan, Jinan 250022, People's Republic of China
[67] University of Manchester, Oxford Road, Manchester, M13 9PL, United Kingdom
[68] University of Muenster, Wilhelm-Klemm-Strasse 9, 48149 Muenster, Germany
[69] University of Oxford, Keble Road, Oxford OX13RH, United Kingdom
[70] University of Science and Technology Liaoning, Anshan 114051, People's Republic of China
[71] University of Science and Technology of China, Hefei 230026, People's Republic of China
[72] University of South China, Hengyang 421001, People's Republic of China

[73] University of the Punjab, Lahore-54590, Pakistan
[74] University of Turin and INFN, (A)University of Turin, I-10125, Turin, Italy; (B)University of Eastern Piedmont, I-15121, Alessandria, Italy; (C)INFN, I-10125, Turin, Italy
[75] Uppsala University, Box 516, SE-75120 Uppsala, Sweden
[76] Wuhan University, Wuhan 430072, People's Republic of China
[77] Yantai University, Yantai 264005, People's Republic of China
[78] Yunnan University, Kunming 650500, People's Republic of China
[79] Zhejiang University, Hangzhou 310027, People's Republic of China
[80] Zhengzhou University, Zhengzhou 450001, People's Republic of China

[a] Also at the Moscow Institute of Physics and Technology, Moscow 141700, Russia
[b] Also at the Novosibirsk State University, Novosibirsk, 630090, Russia
[c] Also at the NRC "Kurchatov Institute", PNPI, 188300, Gatchina, Russia
[d] Also at Goethe University Frankfurt, 60323 Frankfurt am Main, Germany
[e] Also at Key Laboratory for Particle Physics, Astrophysics and Cosmology, Ministry of Education; Shanghai Key Laboratory for Particle Physics and Cosmology; Institute of Nuclear and Particle Physics, Shanghai 200240, People's Republic of China
[f] Also at Key Laboratory of Nuclear Physics and Ion-beam Application (MOE) and Institute of Modern Physics, Fudan University, Shanghai 200443, People's Republic of China
[g] Also at State Key Laboratory of Nuclear Physics and Technology, Peking University, Beijing 100871, People's Republic of China
[h] Also at School of Physics and Electronics, Hunan University, Changsha 410082, China
[i] Also at Guangdong Provincial Key Laboratory of Nuclear Science, Institute of Quantum Matter, South China Normal University, Guangzhou 510006, China
[j] Also at MOE Frontiers Science Center for Rare Isotopes, Lanzhou University, Lanzhou 730000, People's Republic of China
[k] Also at Lanzhou Center for Theoretical Physics, Lanzhou University, Lanzhou 730000, People's Republic of China
[l] Also at the Department of Mathematical Sciences, IBA, Karachi 75270, Pakistan

A light scalar X_0 or vector X_1 particles have been introduced as a possible explanation for the $(g-2)_\mu$ anomaly and dark matter phenomena. Using $(8.998 \pm 0.039) \times 10^9$ J/ψ events collected by the BESIII detector, we search for a light muon philic scalar X_0 or vector X_1 in the processes $J/\psi \to \mu^+\mu^- X_{0,1}$ with $X_{0,1}$ invisible decays. No obvious signal is found, and the upper limits on the coupling $g'_{0,1}$ between the muon and the $X_{0,1}$ particles are set to be between 1.1×10^{-3} and 1.0×10^{-2} for the $X_{0,1}$ mass in the range of $1 < M(X_{0,1}) < 1000$ MeV/c^2 at 90% confidence level.

The Standard Model (SM) of particle physics has achieved remarkable successes as a highly predictive theory of fundamental particles and their interactions. Nonetheless, the SM is generally considered incomplete since it is unable to explain several important questions, anomalies, and phenomena [1–3]. One of the possible experimental evidences of physics beyond the SM is the persistent discrepancy of more than 3σ between the experimental observation and the SM prediction of the muon anomalous magnetic moment $(g-2)_\mu$ [4–6].

Extra $U(1)$ groups have been added as minimal extensions to the SM to study new physics [7, 8]. One of the notable extensions of the SM gauge group is the anomaly-free gauged $U(1)_{L\mu-L\tau}$ model [9–11]. This model introduces a new massive vector boson X_1, which only couples to the second and third generations of leptons $(\mu, \nu_\mu, \tau, \nu_\tau)$ with the coupling strength g'_1. The X_1 can contribute to the muon anomalous magnetic moment and explain the $(g-2)_\mu$ anomaly [12]. Henceforth, we refer to the $U(1)_{L\mu-L\tau}$ model, where X_1 only couples to the SM particles, as the "vanilla" $U(1)_{L\mu-L\tau}$ model. The existence of dark matter (DM) and its observed abundance is one of the greatest mysteries in physics. Recent studies have revealed that an extended $U(1)_{L\mu-L\tau}$ model, which introduces a dark matter particle with mass $M(\chi)$ and coupling to MeV-scale X_1 with the coupling strength g'_D, can also explain DM phenomena and the relic abundance of DM [13–17]. For $M(\chi) < M(X_1)/2$ and coupling ratios $g'_D/g'_1 \gg 1$, the dominant decay mode of the X_1 is invisible, $X_1 \to \chi\bar{\chi}$. We henceforth refer to the model with $\mathcal{B}(X_1 \to \chi\bar{\chi}) \approx 1$ as the "invisible" $U(1)_{L\mu-L\tau}$ model. In addition to a vector boson scenario, an extra $U(1)$ group involving a new light scalar boson X_0, coupling to muons with coupling strength g'_0, has been recently addressed [18–20]. This model can also serve as one possible explanation for the $(g-2)_\mu$ discrepancy within a specific $X_0 - g'_0$ parameter space. In the following, this model is denoted as "scalar" $U(1)$ model.

Stringent constraints on the visible decay of $X_1 \to \mu^+\mu^-$ have been obtained in the BaBar [21], CMS [22] and Belle [23] experiments. The parameter space with $10^{-3} < g'_1 < 1$ in the mass range from the

$\mu^+\mu^-$ threshold to 68 GeV/c^2 has been excluded. Moreover, since the "vanilla" $U(1)_{L\mu-L\tau}$ model modifies the neutrino interactions, there are also strong constraints on the g_1' coupling from neutrino trident $\nu N \to \nu N \mu^+\mu^-$ scattering experiments [24–27]. Therefore, X_1 could weakly couple to the SM particles and predominately decay to invisible final states, especially when the mass of $X_{0,1}$ is below $2m_\mu$. Recently, the invisible decays of X_1 have been investigated in the NA64-e [28] and Belle II [29, 30] experiments. There is no direct result on the scalar boson X_0, but it could be estimated based on the vector scheme [19]. BESIII offers significant advantages in searching for the low-mass $X_{0,1}$ particles via the $J/\psi \to \mu^+\mu^- X_{0,1}$ decay, where the $X_{0,1}$ is radiated from one of the muons and then decays invisibly. First, BESIII has collected a large J/ψ data sample at the e^+e^- center-of-mass energy $\sqrt{s} = 3.097$ GeV [31]. The corresponding cross section of $J/\psi \to \mu^+\mu^- X_{0,1}$ is approximately 22 times greater than that of the continuum $e^+e^- \to \mu^+\mu^- X_{0,1}$ process, which was previously employed in the search for X_1 at Belle II [20]. Second, the lower e^+e^- collider energy at BESIII leads to a better detection resolution, enabling a finer binning scheme in search of low-mass $X_{0,1}$. Additionally, the very narrow width of J/ψ results in a lower background level from the initial state radiation process. Hence, $J/\psi \to \mu^+\mu^-$ offers an ideal opportunity to search for muonic new physics particles [20].

In this Letter, we perform a search for a light muon philic scalar X_0 or vector X_1 in the processes of $J/\psi \to \mu^+\mu^- X_{0,1}$ with $X_{0,1} \to$ invisible, in the mass range from 1 to 1000 MeV/c^2, based on the data sample of 9 billion J/ψ events collected by the BESIII detector in 2009, 2018, and 2019 [31]. The data collected in 2012 is not used because information from the muon counter detectors is unavailable. Three SM extension models, including the "vanilla" $U(1)_{L\mu-L\tau}$ model, the "invisible" $U(1)_{L\mu-L\tau}$ model and the "scalar" $U(1)$ model, are considered. In the "vanilla" $U(1)_{L\mu-L\tau}$ model, X_1 decays to neutrinos with the branching fraction $\mathcal{B}(X_{0,1} \to \nu\bar{\nu})$ varying from 33% to 100% depending on the X_1 mass [32]. In the "invisible" $U(1)_{L\mu-L\tau}$ model, X_1 predominately decays into light DM particles with a branching fraction $\mathcal{B}(X_1 \to \chi\bar{\chi}) \simeq 1$. In the "scalar" $U(1)$ model, X_0 is long-lived with displaced decay or predominately decays to invisible particles. For all models, it is assumed that the total width of the $X_{0,1}$, $\Gamma_{X_{0,1}}$, is negligible compared to the experimental resolution, and set to be zero. Therefore, we look for events with two final state muon tracks with missing energy. In the presence of the $X_{0,1}$ signals, narrow peaks would be visible in the recoil mass distribution of the $\mu^+\mu^-$ system. The branching fractions of the $J/\psi \to \mu^+\mu^- X_{0,1}$, $X_{0,1} \to$ invisible decays are calculated as

$$\mathcal{B}(J/\psi \to \mu^+\mu^- X_{0,1}) \times \mathcal{B}(X_{0,1} \to \text{invisible}) = \frac{N_{\mathrm{X}_{0,1}}}{N_{J/\psi}\epsilon_{\mathrm{X}_{0,1}}}, \quad (1)$$

where $N_{X_{0,1}}$ are the signal yields, $N_{J/\psi} = (8.998 \pm 0.039) \times 10^9$ is the total number of J/ψ events, and $\epsilon_{X_{0,1}}$ are the signal efficiencies for the X_0 and X_1 cases, respectively. The values of the coupling $g_{0,1}'$ can be obtained by converting the results for the branching fractions [20].

The BESIII detector is described in detail elsewhere [33–35]. Simulated Monte Carlo (MC) samples produced with a GEANT4-based [36] package are used to determine detection efficiencies and to estimate backgrounds. The signal events for the $J/\psi \to \mu^+\mu^- X_{0,1}$ with $X_{0,1} \to$ invisible decays are generated based on the theoretical amplitude in Ref. [20] with EVTGEN [37]. We generate signal MC samples at 58 different $X_{0,1}$ mass values with negligible width $\Gamma_{X_{0,1}}$, corresponding to mass hypotheses ranging from 1 to 1000 MeV/c^2 in steps of 10 to 20 MeV/c^2 depending on the resolution. Possible backgrounds are investigated using an inclusive MC sample including the production of the J/ψ resonance and the continuum processes. All particle decays are modeled with EVTGEN using branching fractions either taken from the Particle Data Group [38], when available, or otherwise estimated with LUNDCHARM [39]. The background from $e^+e^- \to \mu^+\mu^-$ events is modelled with BABAYAGA [40]. Final state radiation is simulated with the PHOTOS package [41].

The signal candidates include $\mu^+\mu^-$ tracks and missing energy in the final states. Each charged track is required to be within a polar angle (θ) range of $|\cos\theta| < 0.93$ and the distance of closest approach to the interaction point must be less than 10 cm along the z-axis, and less than 1 cm in the transverse plane. To exclude the cosmic ray events, the momentum of each track is required to be less than 1.55 GeV/c, and the time difference in time-of-flight system (TOF) between two tracks is required to be within $|\Delta t_{\mathrm{TOF}}| < 2$ ns. Events with additional charged tracks reconstructed in the main drift chamber (MDC) are rejected to exclude background from particles with displaced decays, such as K_S^0 and γ-conversion events. Moreover, to distinguish muons from electrons, pions, and kaons, a track is identified as a muon by the following requirements: 1) particle identification (PID) likelihoods, formed by combining the measurements of the energy deposited in the MDC and the flight time in the TOF, satisfy $\mathcal{L}(\mu) > \mathcal{L}(K)$ and $\mathcal{L}(\mu) > 0$, where $\mathcal{L}(\mu)$ and $\mathcal{L}(K)$ are likelihoods calculated based on the muon and kaon hypotheses, respectively; 2) the penetration depth of each track in the muon counters (MUC) is required to exceed $(-40.0 + 70 \times p/(\mathrm{GeV}/c))$ cm for $0.5 \le p \le 1.1$ GeV/c, and to be greater than 40 cm for $p > 1.1$ GeV/c, where p is the momentum of each charged track; 3) the deposited energy in the electromagnetic calorimeter (EMC) ($E_{\mathrm{EMC}}(\mu)$) is required to be within (0.1, 0.3) GeV.

We split the events that pass the above selections into two groups, labeled as low mass region and high mass region. The following selection criteria are optimized for the X_0 and X_1 searches in the low and high mass regions, respectively. In the low mass region, the signals are searched for on the recoil mass squared $RM^2(\mu^+\mu^-) = (p_{J/\psi} - p_{\mu^+} - p_{\mu^-})^2$ distribution since $RM^2(\mu^+\mu^-)$ can be negative due to detector resolution, where the $p_{J/\psi}$ [31], p_{μ^+}, and p_{μ^-} are the four-momenta of J/ψ, μ^+, and μ^- particles, respectively. This region is defined as $RM^2(\mu^+\mu^-) < 0.3$ GeV$^2/c^4$, which is used to search for signals with mass $M(X_{0,1}) < 0.4$ GeV$/c^2$. The dominant backgrounds in this region are composed of two final state muons from the $J/\psi \to \mu^+\mu^-(\gamma)$ and $e^+e^- \to \mu^+\mu^-(\gamma)$ processes, where the photons are from initial and final state radiation. The high mass region is defined as $RM(\mu^+\mu^-) \in [0.25, 1.0]$ GeV$/c^2$ ($RM(\mu^+\mu^-) > 1.0$ GeV$/c^2$ is not studied in this work due to poor understanding of the background) and it is used to search for the signal with mass $M(X_{0,1}) \in [0.4, 1.0]$ GeV$/c^2$ on the recoil mass $RM(\mu^+\mu^-)$ distribution. In addition to the background from $J/\psi \to \mu^+\mu^-(\gamma)$ and $e^+e^- \to \mu^+\mu^-(\gamma)$ processes, a significant background comes from $J/\psi \to K_L^0\pi^\pm K^\mp$ and $J/\psi \to K_L^0\pi^+\pi^-$ decays, where the K_L^0 particle is undetected due to its long decay length.

The common selection criteria for all events are described below. We require the events with the polar angle of the momentum of $\mu^+\mu^-$ system $\cos(\theta_{\mu^+\mu^-})$ within the barrel EMC region $\cos(\theta_{\mu^+\mu^-}) \in [-0.76, 0.76]$, to reject the inefficient region of photon detection. The events within $\cos(\theta_{\mu^+\mu^-}) \in [-0.03, 0.03]$, where photons easily escape due to the crystals being placed perpendicular to the beam direction, are further excluded. Additionally, the invariant mass of $\mu^+\mu^-$ pairs is required to be outside the mass windows of $M(\mu^+\mu^-) \notin [0.429, 0.481]$ GeV$/c^2$ and $M(\mu^+\mu^-) \notin [0.548, 0.780]$ GeV$/c^2$, to further suppress the backgrounds with $K_S^0 \to \pi^+\pi^-$ and $K^* \to K^\pm\pi^\mp$ decays, respectively. The signal processes have two final state muons; to suppress the background with additional final state photons, the total deposited energy in the EMC from all showers ($E_{\rm tot}$(EMC)) in each event is required to be less than 43 MeV (50 MeV) for the low (high) mass region. For these showers, the difference between the EMC time and the event start time is required to be within [0, 700] ns to minimize the impact of electronic noise and showers unrelated to the event. We require the events with opening angle between two muons in the J/ψ rest frame $\cos(\theta_{\mu^+\mu^-})$ to be greater than -0.97 (-0.96) for X_1 (X_0) case in the low mass region, and $\cos(\theta_{\mu^+\mu^-})$ to be greater than -0.97 for both X_1 and X_0 cases in the high mass region, to suppress background from two-body processes of $J/\psi \to \mu^+\mu^-$ and $e^+e^- \to \mu^+\mu^-$ decays. In the high mass region, the background from $J/\psi \to K^\pm K^{*\mp}$ with $K^{*\mp} \to K_L^0\pi^\mp$ decays is suppressed by requiring the recoil mass of $\mu^\pm$, $RM(\mu^\pm)$, to be outside $(0.858, 1.172)$ GeV$/c^2$.

To investigate possible signals from $X_{0,1}$, we perform a series of unbinned maximum likelihood fits to $RM^2(\mu^+\mu^-)$ for the low mass region and to $RM(\mu^+\mu^-)$ for the high mass region. The fits are performed in the mass region of $1 < M(X_{0,1}) < 1000$ MeV$/c^2$, with steps of $10 - 20$ MeV$/c^2$, about half of the signal resolution. The resulting signal efficiency obtained from signal MC samples varies between $1\% - 20\%$ as a function of $M(X_{0,1})$. In the low mass region, the residual backgrounds are from $J/\psi \to \mu^+\mu^-\gamma$, $e^+e^- \to \mu^+\mu^-\gamma$, and $J/\psi \to$ hadrons processes. The yields and probability density functions for the peaking backgrounds from $J/\psi \to \mu^+\mu^-$ and $e^+e^- \to \mu^+\mu^-$ are fixed from the corresponding MC simulation in these fits. The shape of non-peaking background from J/ψ hadronic decays is constructed from the corresponding MC simulation with a yield that is left as a free parameter in the fit. The signal shapes are described as a templated shape constructed from the $X_{0,1}$ signal MC simulations. As an example, Fig. 1 shows the fit results for the $X_{0,1}$ candidates with mass $M(X_{0,1}) = 120$ MeV$/c^2$. For the high mass

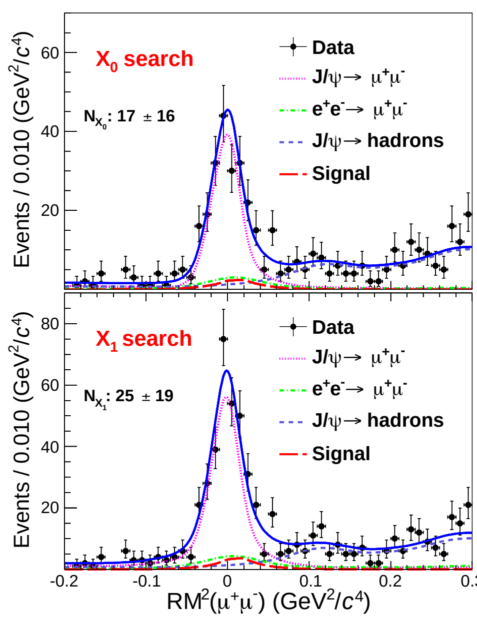

FIG. 1. Fits to the $RM^2(\mu^+\mu^-)$ distributions for the X_0 (top) and X_1 (bottom) candidates with mass $M(X_{0,1}) = 120$ MeV$/c^2$. The red long-dashed curves are the $X_{0,1}$ signal shapes. The green dashed and magenta dotted curves are the peaking backgrounds from $J/\psi \to \mu^+\mu^-, e^+e^- \to \mu^+\mu^-$ processes. Dots with error bars are data, and the blue dashed curves are the backgrounds from $J/\psi \to$ hadrons processes.

region, the signals with mass $M(X_{0,1}) > 0.4$ GeV$/c^2$ are searched for in the $RM(\mu^+\mu^-)$ distribution, and the residual backgrounds are dominated by the J/ψ decays with K_L^0 in the final state, which are described by a second-order Chebychev function. The signal shapes are constructed from the corresponding $X_{0,1}$ signal MC simulations. The fits to the $RM(\mu^+\mu^-)$ distributions with mass $M(X_{0,1}) = 720$ MeV$/c^2$ are shown in Fig. 2. Taking into account the uncertainty from the background model, the maximum local significance among all the fits is determined to be 2.5σ at $M(X_{0,1}) = 720$ MeV$/c^2$, as shown in Fig. 2. The significances are calculated by comparing the likelihoods with and without the signal components in the fit, and considering the change of the number of degrees of freedom. We find no evidence for signals from $X_{0,1}$ invisible decays.

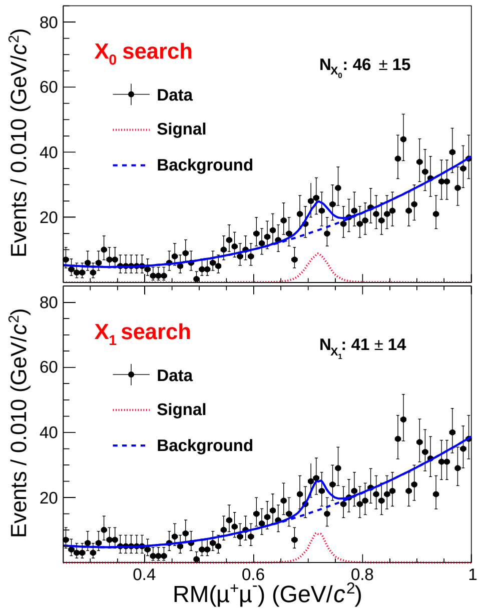

FIG. 2. Fits to the $RM(\mu^+\mu^-)$ distributions for the X_0 (top) and X_1 (bottom) candidates with mass $M(X_{0,1})$ = 720 MeV/c^2. The red dotted curves are the $X_{0,1}$ signal shapes. Dots with error bars are data, and the blue dashed curves describe the combinatorial background contribution. The data points on the two plots are identical due to identical selection criteria for X_0 and X_1.

The systematic uncertainty sources for the coupling $g'_{0,1}$ measurement include the total number of J/ψ events, the signal efficiency, the signal extraction, and the J/ψ total width. The uncertainty from the total number of J/ψ events is 0.4% [31]. The uncertainty from the tracking efficiency is taken as 1.0% per track [42]. The uncertainty associated with the $E_{\mathrm{EMC}}(\mu)$ requirement is 0.2% [42]. The systematic uncertainties from the requirements on Δt_{TOF}, E_{tot}(EMC) and additional tracks in the MDC are estimated with a $J/\psi \to \mu^+\mu^-$ control sample. The resulting differences in the efficiencies between data and MC simulation are 1.0% for Δt_{TOF}, 1.5% for E_{tot}(EMC), and negligible for the requirement on the additional tracks. The uncertainties due to the requirements on PID and MUC penetration depth are investigated with a $J/\psi \to \gamma\mu^+\mu^-$ control sample with tagged photon. The signal MC events are weighted by the difference in efficiency between data and MC simulation. It causes 1.0% and $(1.0-3.0)$% changes in signal efficiencies for PID and penetration depth requirement depending on the mass of $X_{0,1}$. In the fits for the low mass region, the uncertainty from the simulated yields of the peaking background is estimated to be 18.8% and 16.8% for X_0 and X_1, respectively, using the selected $J/\psi \to \gamma\mu^+\mu^-$ control sample. To account for these uncertainties, alternative fits are performed by varying the background yields upwards or downwards by their corresponding uncertainties. For the high mass region, the uncertainty associated with the background model is also considered by an alternative fit with the background described by a third-order polynomial shape. Among these fits, the one with the largest upper limit on the signal yield is treated as the final result. The systematic uncertainty from the resolution difference between data and MC simulation is determined to be 1.0% using a control sample of $J/\psi \to K^0_S K^0_L$ events. Considering that the cross section of the $e^+e^- \to \mu^+\mu^-$ process is 4.4% of the $J/\psi \to e^+e^-$ one [43], and taking into account the efficiency difference between $e^+e^- \to \mu^+\mu^- X_{0,1}$ and $J/\psi \to \mu^+\mu^- X_{0,1}$, the uncertainties for the contributions from the $e^+e^- \to \mu^+\mu^- X_0$ and $e^+e^- \to \mu^+\mu^- X_1$ processes are determined to be 3.5% and 3.9%, respectively. The uncertainty associated with the total width of J/ψ is 1.8% [38]. Assuming all these sources as independent, the total systematic uncertainty is obtained by adding the individual contributions in quadrature, resulting in $(5.0-5.4)$% and $(5.5-5.8)$% for X_0 and X_1, respectively.

Since no obvious signal is observed, the upper limits on the product branching fractions $\mathcal{B}(J/\psi \to \mu^+\mu^- X_{0,1}) \times \mathcal{B}(X_{0,1} \to \text{invisible})$ in Eq. 1 are determined at the 90% confidence level (C.L.) depending on the mass $M(X_{0,1})$ with Bayesian method. A likelihood scan is performed by varying the number of signals in the fit, and the effect of the systematic uncertainty is considered by convolving the likelihood curve with a Gaussian function with its standard deviation set to the total systematic uncertainty. The resulting 90% C.L. upper limits on $\mathcal{B}(J/\psi \to \mu^+\mu^- X_{0,1}) \times \mathcal{B}(X_{0,1} \to \text{invisible})$ are determined to be $6.2\times10^{-9} - 5.5\times10^{-7}$ and $4.5\times10^{-9} - 9.6\times10^{-7}$ for the cases of X_0 and X_1 as functions of $M(X_{0,1})$, respectively. The results on the branching fractions are used to estimate limits on the coupling $g'_{0,1}$ [20]. The excluded region in the $g'_{0,1}$ versus $M(X_1)$ parameter space at the 90% C.L. is shown in Fig. 3. For the "vanilla" $L_\mu - L_\tau$ model, BESIII excludes g'_1 values in the range $1.6\times10^{-3} - 7.9\times10^{-3}$ as a function of $M(X_1)$ after taking $\mathcal{B}(X_1 \to \nu\bar{\nu})$ into account. For the "invisible" scenario, g'_1 values in the range $1.1\times10^{-3} - 5.5\times10^{-3}$ with $1 \leq M(X_1) \leq 1000$ MeV/c^2 are excluded. We obtain a better sensitivity in the range 200 - 860 MeV/c^2 compared to the Belle II results [29, 30], and a comparable upper limit in the lower mass region with a finer binning scheme. The best constraint for the mass region $M(X_1) < 10$ MeV/c^2 is provided in the NA64-e experiment [28]. For the "scalar" X_0 case, there are no earlier experimental measurements; the 90% C.L. upper limits on the coupling g'_0 is determined to be $2.3\times10^{-3} - 1.0\times10^{-2}$ with $M(X_0)$ in the range 1 - 1000 MeV/c^2.

In summary, we have searched for a muon philic scalar X_0 or vector X_1 boson, introduced by many SM extension models, using a data sample of 9 billion J/ψ events

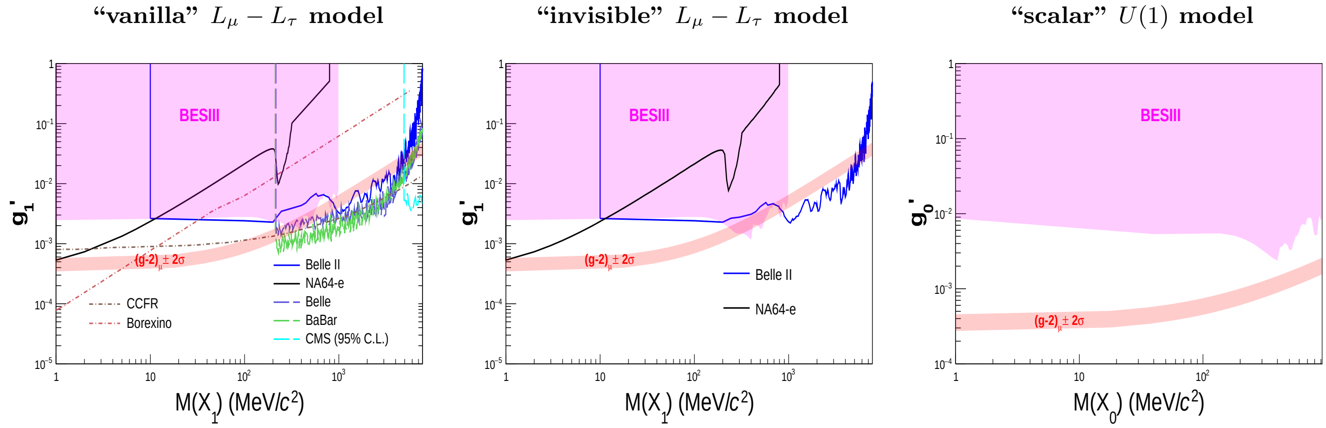

FIG. 3. The 90% C.L. upper limits on the coupling $g'_{0,1}$ for the "vanilla" $L_\mu - L_\tau$ model, the "invisible" $L_\mu - L_\tau$ model, and the "scalar" $U(1)$ model. For the "vanilla" $L_\mu - L_\tau$ model, the previous excluded regions by BaBar [21], CMS [22], and Belle [23] via the $X_1 \to \mu^+\mu^-$ decay and the constraints from neutrino experiments [24–27] are shown for comparison. For the "invisible" $L_\mu - L_\tau$ model, the previous searches for X_1 invisible decays by NA64-e [28] and Belle II [29, 30] are also presented. The red bands represent the parameter regions favored by the $(g-2)_\mu$ anomaly within 2σ [20].

at BESIII. No evidence of $X_{0,1}$ has been observed in the mass range $1 < M(X_{0,1}) < 1000$ MeV/c^2, and the 90% C.L. upper limits on the coupling $g'_{0,1}$ are set to be in the range of $1.1 \times 10^{-3} - 1.0 \times 10^{-2}$ for three SM extension models. To date, we provide the best constraint for the X_1 mass in the range 200 - 860 MeV/c^2 in the "invisible" $L_\mu - L_\tau$ model, and two mass regions within $320 < M(X_1) < 410$ MeV/c^2 and $460 < M(X_1) < 520$ MeV/c^2 are excluded to explain the $(g-2)_\mu$ anomaly at the 90% C.L.. For the scalar X_0, we have performed the first direct experiment search, and set the upper limit at the 90% C.L. on the coupling g'_0 to $2.3 \times 10^{-3} - 1.0 \times 10^{-2}$ for $1 < M(X_0) < 1000$ MeV/c^2.

The BESIII Collaboration thanks the staff of BEPCII and the IHEP computing center for their strong support. This work is supported in part by National Key R&D Program of China under Contracts Nos. 2020YFA0406400, 2020YFA0406300; National Natural Science Foundation of China (NSFC) under Contracts Nos. 11635010, 11735014, 11835012, 11935015, 11935016, 11935018, 11961141012, 12025502, 12035009, 12035013, 12061131003, 12192260, 12192261, 12192262, 12192263, 12192264, 12192265, 12221005, 12225509, 12235017; the Chinese Academy of Sciences (CAS) Large-Scale Scientific Facility Program; the CAS Center for Excellence in Particle Physics (CCEPP); Joint Large-Scale Scientific Facility Funds of the NSFC and CAS under Contract No. U1832207; CAS Key Research Program of Frontier Sciences under Contracts Nos. QYZDJ-SSW-SLH003, QYZDJ-SSW-SLH040; 100 Talents Program of CAS; The Institute of Nuclear and Particle Physics (INPAC) and Shanghai Key Laboratory for Particle Physics and Cosmology; European Union's Horizon 2020 research and innovation programme under Marie Sklodowska-Curie grant agreement under Contract No. 894790; German Research Foundation DFG under Contracts Nos. 455635585, Collaborative Research Center CRC 1044, FOR5327, GRK 2149; Istituto Nazionale di Fisica Nucleare, Italy; Ministry of Development of Turkey under Contract No. DPT2006K-120470; National Research Foundation of Korea under Contract No. NRF-2022R1A2C1092335; National Science and Technology fund of Mongolia; National Science Research and Innovation Fund (NSRF) via the Program Management Unit for Human Resources & Institutional Development, Research and Innovation of Thailand under Contract No. B16F640076; Polish National Science Centre under Contract No. 2019/35/O/ST2/02907; The Swedish Research Council; U. S. Department of Energy under Contract No. DE-FG02-05ER41374.

[1] A. Crivellin and M. Hoferichter, Science **374**, 1051 (2021).
[2] P. J. Fox *et al.*, [arXiv:2210.03075 [hep-ph]].
[3] S. Chen and S. L. Olsen, Natl. Sci. Rev. **8**, nwab189 (2021).
[4] G. W. Bennett *et al.* [Muon g-2 Collaboration], Phys. Rev. D **73**, 072003 (2006).
[5] B. Abi *et al.* [Muon g-2 Collaboration], Phys. Rev. Lett. **126**, 141801 (2021).
[6] D. P. Aguillard *et al.* [Muon g-2 Collaboration], [arXiv:2308.06230 [hep-ex]].
[7] M. Pospelov, Phys. Rev. D **80**, 095002 (2009).
[8] M. Bauer, P. Foldenauer and J. Jaeckel, JHEP **07**, 094 (2018).

[9] R. Foot, Mod. Phys. Lett. A **06**, 527 (1991).
[10] X. G. He, G. C. Joshi, H. Lew and R. R. Volkas, Phys. Rev. D **43**, R22 (1991).
[11] R. Foot, X. G. He, H. Lew and R. R. Volkas, Phys. Rev. D **50**, 4571 (1994).
[12] D. W. P. Amaral, D. G. Cerdeno, A. Cheek and P. Foldenauer, Eur. Phys. J. C **81**, 861 (2021).
[13] A. Kamada, K. Kaneta, K. Yanagi and H. B. Yu, JHEP **06**, 117 (2018).
[14] P. Foldenauer, Phys. Rev. D **99**, 035007 (2019).
[15] Y. Kahn, G. Krnjaic, N. Tran and A. Whitbeck, JHEP **09**, 153 (2018).
[16] S. Patra, S. Rao, N. Sahoo and N. Sahu, Nucl. Phys. B **917**, 317-336 (2017).
[17] B. Shuve and I. Yavin, Phys. Rev. D **89**, 113004 (2014).
[18] C. Y. Chen, M. Pospelov and Y. M. Zhong, Phys. Rev. D **95**, 115005 (2017).
[19] R. Capdevilla, D. Curtin, Y. Kahn and G. Krnjaic, JHEP **04**, 129 (2022).
[20] G. Cvetič, C. S. Kim, D. Lee and D. Sahoo, JHEP **10**, 207 (2020).
[21] J. P. Lees *et al.* [BaBar Collaboration], Phys. Rev. D **94**, 011102 (2016).
[22] A. M. Sirunyan *et al.* [CMS Collaboration], Phys. Lett. B **792**, 345-368 (2019).
[23] T. Czank *et al.* [Belle Collaboration], Phys. Rev. D **106**, 012003 (2022).
[24] W. Altmannshofer, S. Gori, M. Pospelov and I. Yavin, Phys. Rev. Lett. **113**, 091801 (2014).
[25] A. Kamada and H. B. Yu, Phys. Rev. D **92**, 113004 (2015).
[26] S. Gninenko and D. Gorbunov, Phys. Lett. B **823**, 136739 (2021).
[27] M. Atzori Corona, M. Cadeddu, N. Cargioli, F. Dordei, C. Giunti, Y. F. Li, E. Picciau, C. A. Ternes and Y. Y. Zhang, JHEP **05**, 109 (2022).
[28] Y. M. Andreev *et al.* [NA64 Collaboration], Phys. Rev. D **106**, 032015 (2022).
[29] I. Adachi *et al.* [Belle II Collaboration], Phys. Rev. Lett. **124**, 141801 (2020).
[30] I. Adachi *et al.* [Belle II Collaboration], Phys. Rev. Lett. **130**, 231801 (2023).
[31] M. Ablikim *et al.* [BESIII Collaboration], Chin. Phys. C **46**, 074001 (2022).
[32] T. Araki, S. Hoshino, T. Ota, J. Sato and T. Shimomura, Phys. Rev. D **95**, 055006 (2017).
[33] M. Ablikim *et al.* [BESIII Collaboration], Nucl. Instrum. Meth. A **614**, 345 (2010).
[34] X. Li *et al.*, Radiat. Detect. Technol. Methods **1**, 13 (2017); Y. X. Guo *et al.*, Radiat. Detect. Technol. Methods **1**, 15 (2017); P. Cao *et al.*, Nucl. Instrum. Meth. A **953**, 163053 (2020).
[35] K. X. Huang *et al.*, Nucl. Sci. Tech. **33**, 142 (2022).
[36] S. Agostinelli *et al.* [GEANT4 Collaboration], Nucl. Instrum. Meth. A **506**, 250 (2003).
[37] D. J. Lange, Nucl. Instrum. Meth. A **462**, 152 (2001); R. G. Ping, Chin. Phys. C **32**, 599 (2008).
[38] R. L. Workman *et al.* [Particle Data Group], Prog. Theor. Exp. Phys. 2022, 083C01 (2022).
[39] J. C. Chen, G. S. Huang, X. R. Qi, D. H. Zhang and Y. S. Zhu, Phys. Rev. D **62**, 034003 (2000); R. L. Yang, R. G. Ping and H. Chen, Chin. Phys. Lett. **31**, 061301 (2014).
[40] C. M. Carloni Calame, G. Montagna, O. Nicrosini and F. Piccinini, Nucl. Phys. B Proc. Suppl. **131**, 48-55 (2004).
[41] E. Richter-Was, Phys. Lett. B **303**, 163 (1993).
[42] M. Ablikim *et al.* [BESIII Collaboration], Phys. Rev. D **105**, 012008 (2022).
[43] D. M. Asner *et al.*, Int. J. Mod. Phys. A **24**, S1-794 (2009).